

Numerical simulation of a passive optical Q – switched solid state laser – high brightness Nd:YAG laser case

I. LANCRANJAN*, S. MICLOS^a, D. SAVASTRU^a

*Advanced Study Center–National Institute of Aerospace Research “Elie Carafoli”,
220 Iuliu Maniu Boulevard, Bucharest, Romania

^a National Institute R&D of Optoelectronics, INOE 2000, 409 Atomistilor str.,
P. O. Box MG. 5, Magurele-Ilfov, Romania

This paper is the first of a series on numerical simulation of solid state lasers operated in passive optical Q-switching regime and their applications in various fields. The main purpose of this series is to present the results obtained using numerical analysis as a tool for properly designing solid state lasers, function of application for which these are dedicated since the passive optical Q-switching regime is a large scale used technique. In this paper the numerical simulation results obtained for a passive optical Q-switched Nd:YAG laser of a smaller volume dedicated to ~ 5ns FWHM time duration and over 200 mJ energy pulse generation. The main purpose of the performed theoretical analysis consists of a better understanding of Nd:YAG laser q-switching process itself and of its possible applications in range finding, guiding, materials micro processing and nonlinear optics.

(Received May 11, 2011; accepted May 25, 2011)

Keywords: Passive optical Q-switching, Numerical simulation, Nd:YAG laser, Laser application

1. Introduction

This paper is the first of a series pointing to reach an improved design methodology of solid state lasers operated in passive optical Q-switching regime and dedicated for various civilian and military applications. The main purpose of this first paper is to report the numerical simulation and experimental results obtained in investigating high brightness Nd:YAG lasers operated in passive optical Q-switching regime using LiF:F₂⁻ crystals [3]-[5]. The numerical simulation results are obtained using the coupled rate equations approach, which, even if it is used for a long time, it is still useful in order to gather information necessary for an improved design [1-7,18,19,21,22]. In performing the numerical analysis of the specified laser case, both threshold conditions for attaining Q-switching process are analyzed [1-7]. The numerical simulation results are compared with experimental ones, in order to certify the developed computing procedures, being observed a fairly good agreement between these two categories of results.

2. Theory

A set of three coupled rate equations was proposed by Siegman to model a solid-state laser passively Q-switched by a saturable absorber [1]. This set of coupled differential equations is pointing to investigate a laser oscillator based on an active medium coupled with a saturable absorber, such as the one schematically presented in Fig.1. In Fig. 1 the active medium can be observed, with electronic energy levels denoted as am0 - ground level, am1- pump band, am2 - the upper laser level, am3 - the lower laser level and

the saturable absorber, of which functional cycle can be described using the electronic energy levels sa1 - ground level, sa2 - the upper saturable absorber level, sa3 – the saturable absorber lower excited state, sa4 - the saturable absorber upper excited state. In Fig. 1 the well-known “4 – levels” scheme describing the active medium operation can be observed. The improvement introduced by Siegman and others [1,6-10] consisted into considering possible non-saturable parasitic absorption of the Q-switch cell at laser wavelength, this electronic transition being represented by the sa3 → sa4 absorption.

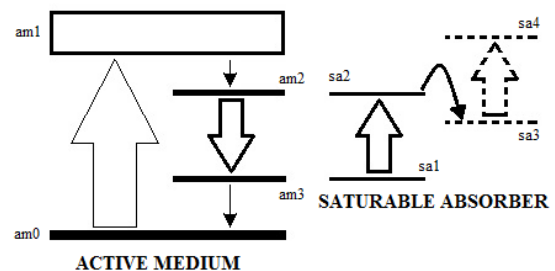


Fig.1. The schematic of a solid state laser operated in passive optical Q-switched regime. Active medium - levels: am0 - ground level; am1- pumping level; am2 - upper laser level; am3 - lower laser level; Saturable absorber - sa1 - ground level; sa2 - upper saturable absorber level; sa3 - saturable absorber lower excited level; sa4 –

saturable absorber upper excited level.

The considered set of these rate equations, with an improvement which consists of the fact that they are modi-

fiation herein to be also included and the population reduction factor of the laser are defined as [1], [6]-[15]:

$$\frac{dn}{dt} = K_g N_g n - K_a N_a n - \beta K_a (N_{a0} - N_a) n - \gamma_c n \quad (1)$$

$$\frac{dN_g}{dt} = R_p - \gamma_g N_g - \gamma K_g N_g n \quad (2)$$

$$\frac{dN_a}{dt} = \gamma_a (N_{a0} - N_a) - K_a N_a n \quad (3)$$

In Equations (1), (2) and (3), the considered laser oscillator parameters are defined as:

- n - the photon number in the laser cavity;
- N_g - the population inversion of the laser active medium, defining the gain of the laser oscillator;
- N_a - the ground-state population of the saturable absorber;
- N_{a0} - the initial value of N_a , being virtually the concentration of saturable absorption centers.

In Equations (1), (2) and (3), the following parameters are introduced:

- K_g - coupling coefficient for laser photons and active centres of the laser active medium;
- K_a - coupling coefficient for laser photons and passive saturable absorber centers of the passive optical Q-switch;
- R_p - the pumping rate of the active medium;
- γ_c - the effective laser cavity decay rate;
- γ_g - the effective decay rate of the upper laser level;
- γ - a coefficient depending on active medium energy-level diagram (2 for three energy-level case, 1 in the four level case);
- γ_a - the coefficient of saturable - absorber relaxation rate;
- β - the ratio of excited state absorption cross section to ground state absorption cross section.

The coupling coefficients introduced in Equations (1), (2) and (3) depend on active medium and passive optical Q-switch cell spectroscopic and geometrical characteristics. For the active medium, the coupling coefficient is defined as:

$$K_g = \frac{2\sigma_g}{\tau_r A_g} \quad (4)$$

where σ_g is the laser emission cross section, τ_r is the cavity round-trip transit time and A_g is the effective laser beam area on the laser gain medium. In the case of saturable absorber, the coupling coefficient is defined as:

$$K_a = \frac{2\sigma_a}{\tau_r A_a} \quad (5)$$

where σ_a is the saturable absorber's ground-state absorption cross section at the laser wavelength and A_a is the effective laser beam area on the saturable absorber. In

Equations (4) and (5), the cavity round-trip transit time, τ_r is defined as:

$$\tau_r = \frac{2l_r}{c} \quad (6)$$

where l_r is the laser resonator length and c is the speed of light.

In equations (1), (2) and (3), γ_c denotes the laser cavity decay rate, defined as:

$$\gamma_c = \frac{1}{\tau_c} \quad (7)$$

where τ_c is the cavity lifetime of the laser photons, being a measure of the existing losses. γ_g is the effective decay rate of the upper laser level, being defined as:

$$\gamma_g = \frac{1}{\tau_g} \quad (8)$$

where τ_g is the laser's emission lifetime, the upper laser level fluorescence lifetime. γ_a is the saturable absorber's spontaneous relaxation rate, being defined as:

$$\gamma_a = \frac{1}{\tau_a} \quad (9)$$

where τ_a is the saturable absorber's fluorescence emission lifetime. β is defined as:

$$\beta = \frac{\sigma_{ESA}}{\sigma_a} \quad (10)$$

where σ_{ESA} is the excited-state absorption cross section of the saturable absorber.

The analysis of a passive optical Q-switched solid state laser can be simply performed by numerical integration of coupled differential equations system (1), (2) and (3). Important characteristics of a saturable absorber Q-switched laser system can be found by analyzing these three coupled-rate equations. Following the method of Siegman [1] and considering the hypothesis of passive Q switching with a slow-relaxing saturable absorber, from Eq. (1), after some algebraic manipulation, the following relation is obtained:

$$\frac{1}{n} \frac{dn}{dt} \cong \gamma_{g0} + \left(K_a^2 N_{a0} - \gamma K_g^2 N_{g0} \right) \frac{n}{\gamma_{g0}} \quad (11)$$

In Eq. (11), γ_{g0} represents "an initial gain" coefficient of the laser oscillator before the start of Q-switching process and is defined as:

$$\gamma_{g0} = K_g N_{g0} - K_a N_{a0} - \gamma_c \quad (12)$$

In the equations (11) and (12), N_{g0} is the laser population inversion required for laser action, the N_g initial value when considering the "start" of laser oscillation in free-running regime, defined as:

$$N_{g0} \cong \frac{K_a N_{a0} + \gamma_c}{K_g} \quad (13)$$

Two important observations have to be made when analyzing equation (11), regarding the Q-switching process, namely that there are two threshold conditions to be fulfilled:

- Initially, before starting the Q-switching, the photon number is small and the photon number's growth rate is dominated by the first term on the right hand side of expression (11); i.e. γ_{g0} . Thus, before the absorber saturation, in atto or picoseconds timing, the photon number inside the laser resonator increases at an initial growth rate γ_{g0} .
- When the photon number is large, the second term starts to take control. Therefore, for the passive Q switching to really occur, both these terms have to be positive. As necessary, it is introduced a second threshold condition for Q-switching. The threshold population inversion after the saturation of the Q switch, N_{th} , is defined as:

$$N_{gth} \cong \frac{\beta K_a N_{a0} + \gamma_c}{K_g} \quad (14)$$

To compare the population inversion of the laser with the loss of the overall laser system when interpreting the numerical simulation results, it is convenient to define a normalized loss parameter, Loss, from Eq. (1) as:

$$Loss = \frac{K_a N_a + \beta K_a (N_{a0} - N_a) + \gamma_c}{K_g} \quad (15)$$

An important feature of the performed numerical analysis consists in investigating the LiF:F₂⁻ passive optical Q-switches functional cycle. The saturable absorption centers of the investigated passive optical Q-switches, the LiF:F₂⁻ crystals, are the F₂⁻ color centers defined as double adjacent anionic vacancies, which captured three electrons. It can be compared with a single ionized hydrogen molecule with diffuse nuclei.

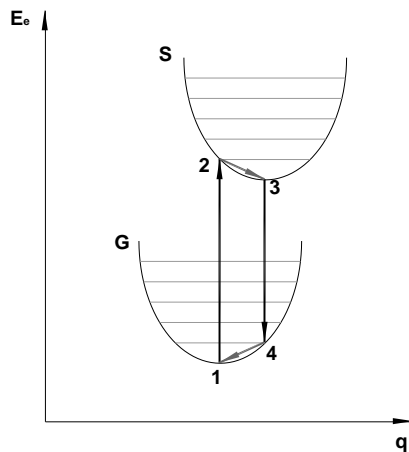


Fig. 2. The functional cycle of F₂⁻ color centers. q - generalised coordinate; E_e - electronic energy level; G - the ground electronic state; S - the first excited electronic state.

The F₂⁻ color center functional cycle can be defined into a Franck - Condon diagram, describing the electronic energy levels and optical transitions of the F₂⁻ color centers, as schematically presented in Fig. 2.

- 1 → 2 - electric dipole electronic - vibrational absorptive transition. It corresponds to an absorption band centered at $\lambda_M = 0.96 \mu\text{m}$ with a half amplitude bandwidth $\tilde{\nu}_{0.5}$ of $1400 \div 1700 \text{ cm}^{-1}$ (at room temperature, $T=300\text{K}$)
- 2 → 3 - vibrational relaxation to the minimum of the S potential energy curve. It is accompanied by a mutual rearrangement of the neighboring ions or by phonon emission. It has a characteristic lifetime of $10^{-12} \div 10^{-13} \text{ s}$.
- 3 → 4 - emissive electron-vibrational transition with a characteristic lifetime τ_a of $60 \div 100 \text{ ns}$. It corresponds to a large fluorescence band situated in the spectral range $1.14 \div 1.28 \mu\text{m}$.
- 4 → 1 - vibrational relaxation to the minimum of the G potential energy curve. It is accompanied by a mutual rearrangement of the neighboring ions or by phonon emission. It has a characteristic lifetime of $10^{-12} - 10^{-13} \text{ s}$.

According to these information, obtained from literature and by direct spectroscopic measurements, the LiF:F₂⁻ passive optical Q-switches show no non-saturable parasitic absorption at operating laser wavelength ($\lambda_L = 1.064 \mu\text{m}$).

4. Numerical simulation results

Using the developed numerical simulation programs, for all three investigated LiF:F₂⁻ Q-switch samples, denoted as C41, C75 and C102, for both experiment lines an, similar procedures are followed. These procedures are performed in three steps:

- Evaluation of the parameters entering in Eqs. (1), (2) and (3) by using equations (4) – (9).
- Numerical solving the differential coupled equations (1), (2) and (3) on pursuit of obtaining a laser pulse time shape, active medium population inversion and loss variation.
- Basic analysis and validation of the performed numerical simulation results by comparison with experimental ones.

The geometrical and spectroscopic characteristics of the investigated LiF:F₂⁻ Q-switch samples are presented in Table 3. Their chemical characteristics, more precisely, the impurity content concentrations and the irradiation processing techniques used for obtaining F₂⁻ color centers are described in Tables 1 and 2.

In the following the results of numerical simulation performed for the “best” and the “worst” experimentally observed results are presented. The “best” are considered the experimental results obtained at CONTINUUM Laser Laboratory by using C102 sample. The “worst” is considered the case of C75 sample used in a previous experiment.

For both “best” and “worst” cases, several parameters introduced in equations. (1), (2) and (3) have similar values:

- The active media used in the experiment lines have the same \varnothing 6mm diameter. This means that A_g , the effective laser beam area on the laser gain medium, has the same value, $A_g = 0.283 \text{ cm}^2$.
- No focalization on the passive optical Q-switches was necessary in both line of experiments, as a consequence, A_a the effective laser beam area on the saturable absorber is considered as equal to A_g .
- The LiF:F₂⁻ crystals absorption cross section at laser wavelength is defined as $\sigma_a = 1.56 \times 10^{-17} \text{ cm}^2$ [16], .
- The F₂⁻ color centers upper level fluorescence lifetime is defined as $\tau_a = 75 \text{ ns}$ [16], [20].
- The laser emission cross section, σ_g is defined as $\sigma_g = 6.5 \times 10^{-19} \text{ cm}^2$ [2],[3].

The length of the laser resonators are a little different, $l_r = 0.400 \text{ m}$ in the case of C102 sample and $l_r = 0.435 \text{ m}$ in the case of C75 sample. The round-trip transit time, τ_r is considered as the same for both lines of experiments, $\tau_r = 2.669 \text{ ns}$ in the first case and $\tau_r = 3.302 \text{ ns}$ in the second one.

In the “best” case, using C102, the coupling coefficients are defined as $K_g = 1.723 \times 10^{-9}$ and $K_a = 4.135 \times 10^{-8}$. In the “worst” case, when using C75, the considered coupling coefficients are practically the same, having insignificant differences: $K_g = 1.723 \times 10^{-9}$ and $K_a = 4.135 \times 10^{-8}$.

The initial value of population inversion is evaluated using a relation derived from Eq. (13):

$$N_{g0} = \frac{-\ln(R_1) - \ln(R_2) - 2\ln(T_{Lin})}{\sigma_g l_{MA}} \quad (16)$$

where T_{Lin} is the small signal (initial) value of Q-switch crystal transmittance at laser wavelength, R_1 and R_2 are the back mirror and output coupler reflectivities and l_{MA} is the pumped length of the active medium. In the “best” care of sample C102, $l_{MA} = 10 \text{ cm}$ and $N_{g0} = 1.192 \times 10^{18}$. For the “worst” case of sample C75, the similar values are: $l_{MA} = 6 \text{ cm}$ and $N_{g0} = 2.060 \times 10^{18}$.

The parameters related to passive optical Q-switch crystal are evaluated by a formula using the results obtained by spectroscopic and absorption laser saturation experiments [21]:

$$N_{a0} = \frac{-\ln\left(\frac{T_{Lin}}{T_{Lfin}}\right)}{\sigma_a l_a} \quad (17)$$

where T_{Lfin} is the large, saturation signal (final - saturated) value of Q-switch crystal transmittance at laser wavelength and l_a is the length of the Q-switch crystal. For C102 these values are: $l_a = 3.0 \text{ cm}$ and $N_{a0} = 5.767 \times 10^{16}$. For C75, the similar values are $l_a = 4.7 \text{ cm}$ and $N_{a0} = 3.621 \times 10^{16}$.

The system of coupled rate equations (1), (2) and (3) is solved using a Runge-Kutta-Fehlberg algorithm (RKF45). The coefficient depending on active medium energy-level diagram is considered as unitary, $\gamma = 1$. The observed numerical simulation results for both the “best” and the “worst” cases, using the previously defined parameters introduced in equations. (1), (2) and (3), are presented in

Fig. 3, 4, 5, 6. $R_p \cong 1.5 \times 10^{20}$ for the “best” case of Sample C102, being approximated using observed experimental results obtained for free-running regime. $R_p \cong 1.7 \times 10^{19}$ using the same procedure.

For both the “best” and the “worst” cases, the parameter β is considered as extremely low, practically zero by applying a first comparison criterion of laser pulse full-width half measure time width observed experimentally and by numerical simulation. The second criterion consists in comparison of experimentally observed value of laser single pulse output energy in Q-switching regime with the total value of emitted laser photons obtained by numerical integration of the photon density curves presented in Figs. 3 and 5. The observed differences between these two kinds of results is less than 10% for both investigated “best” and “worst” cases. The observed value of β is in agreement with spectroscopic measurements performed experimentally and reported in literature [17], [20]. According to these information, the LiF:F₂⁻ crystals exhibit no parasitic non-saturable absorption at laser wavelength from an excited level sa3, as in Fig.1.

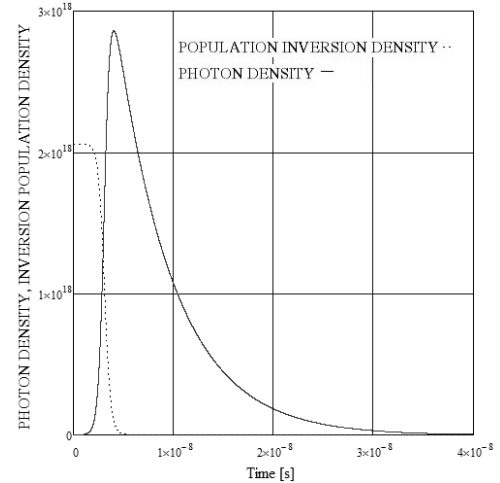


Fig. 3. The numerical simulation results observed in the “best” case of Sample C102. The photon density and population inversion density curves.

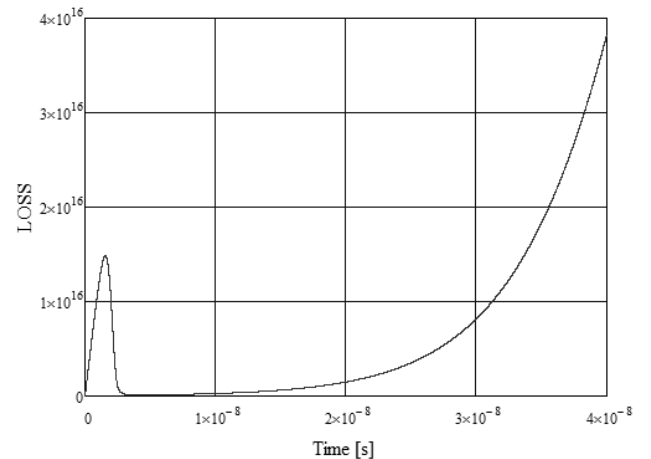


Fig. 4. The numerical simulation results observed in the “best” case of Sample C102. The LOSS curve.

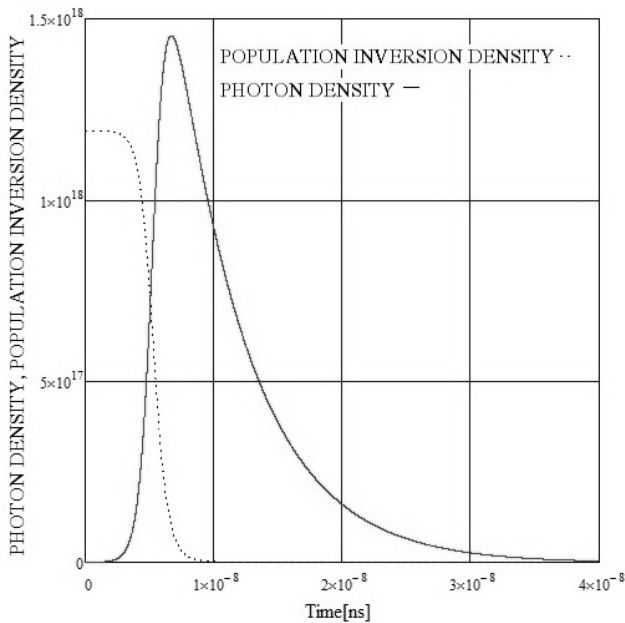


Fig. 5. The numerical simulation results observed in the “worst” case of Sample C75. The photon density and population inversion density curves.

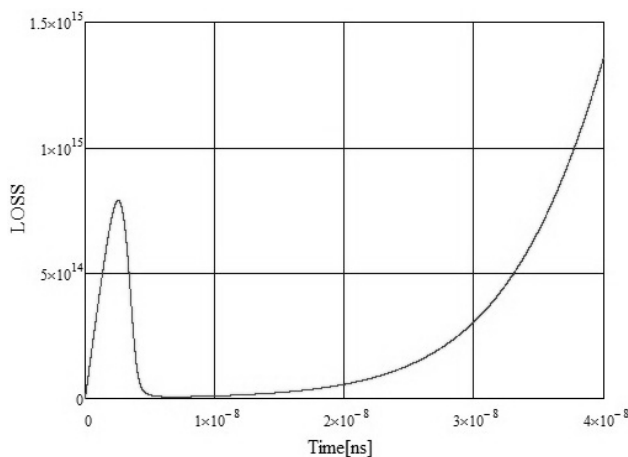


Fig. 6. The numerical simulation results observed in the “worst” case of Sample C75. The LOSS curve.

In the “best” case of Sample C102 the full-width half measured (FWHM) laser single pulse time duration is estimated as 5.5 ns. For the “worst” C75 case the full-width half measured (FWHM) laser single pulse time duration is estimated as 6.0 ns.

For both the “best” and the “worst” cases the parameter, the initial photon density value $n(0)$ is approximated as 10^{14} . It is a rough approximation of the fluorescence emission of Nd:YAG laser active medium and laser resonator geometries almost identical for both lines of experiments.

Regarding the numerical simulation results presented in Figs. 4 and 6, the LOSS curves for the “best” C102 and “worst” C75 cases, several observations can be made:

- The presented numerically obtained curves are, in both cases, with a scale factor, identical with the $N_a(t)$ ones, as expected for $\beta = 0$.

- The initial increase of $N_a(t)$ is considered to be due to the passive Q-switching mechanism, being explained by the different moments of attaining the two first and the second thresholds for proper Q-switching operation.

5. Experimental setup

The numerical simulation results are compared with the experimental ones obtained with two lines of experiments, which were performed for the Sample C75 (the schematic of the developed experimental setup is presented in Fig. 7) and for the Sample C102 (the schematic of the developed experimental setup is presented in Fig. 8).

Both experimental setups are developed on the basic idea to construct a passively Q-switched Nd:YAG laser oscillator emitting light pulses with few nanoseconds FWHM time duration and as large output energy as possible by using a short laser resonator and large contrast LiF:F₂⁻ passive optical Q-switches.

The experimental setup developed for the Sample C75 consists of a plane-plane 43.5 cm length resonator with high reflectivity (HR in Fig. 7) of 0.99 reflection coefficient and output coupler (OC in Fig. 7) manufactured of a quartz plate of 0.08 reflection coefficient. Into the laser resonator, in order to improve the stability laser output stability, a polarizer is inserted made of a 1 mm thick quartz plate placed at Brewster angle versus optical axis. The cylindrical LiF:F₂⁻ passive optical Q-switch cell is mounted approximately at one third of the laser resonator. The LiF:F₂⁻ has no dielectric AR coatings on the optical plane parallel (less than 30° error) end faces. The pumping system consists of a QUANTRON 104 B reflector made of a cylindrical Quartz block with external and the two internal holes for flash lamp and active medium optical quality polished surfaces. QUANTRON 104 B reflector is made of a colloidal silver layer chemically deposited on the external surface Quartz block surface and protected from oxidation by an electrochemically deposited Ni-Cu layer. An INP 5/60 AI flash lamp mounted on a power source which injected discharge current of ~ 200 μs duration is used. The adjustable repetition frequency of flash lamp pumping pulses is set at 12.5 pps (Hz). The active medium is a Ø 6×80 mm Nd:YAG laser rod with both ends having AR coatings. The active medium is pumped on 60 mm of its length. The QUANTRON 104 B reflector, flash lamp and laser rod are cooled with flowing de-ionized water.

The laser output is measured with a system composed of:

- laser energy measurement - a thermoelectric GENTEC ED2S energy meter used as the “calibration unit” and a silicon photodiode ROL 021 operated in an inverse polarization mode as a service laser energy monitor;
- laser pulse time shape measurement - an ITT F4014 vacuum photodiode (~ 10 ps response time) coupled to a Tektronix 519 oscilloscope (1GHz bandwidth). The response time of this measuring system was estimated as ~ 1 ns.

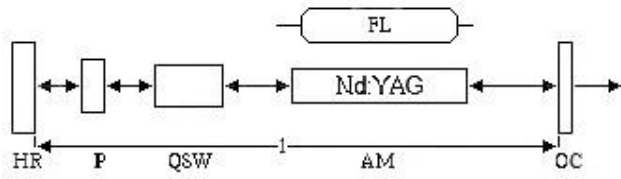


Fig. 7. Schematic representation of the investigated high brightness Nd:YAG laser setup developed for Sample C75. HR - High Reflectivity back mirror; P - Polarizer; QSW - LiF:F₂⁻ passive optical Q-switch cell; AM - active medium; OC - output coupler

The experimental setup developed for Sample C102 consists of a 40 cm long resonator, using a high reflectivity concave (+ 4 m) mirror and an output coupler made of a variable reflectivity mirror (VRM) with Gaussian distribution with 0.12 peak reflectivity and a spot of 1.2 mm. As pumping chamber, it was used a double flash lamp CONTINUUM 711-06 laser head. A 1.1% concentration $\varnothing 6 \times 115$ mm Nd:YAG rod was used as the active medium. The flash lamps and the active medium are cooled with flowing de-ionized water. The pumped length of the active medium is considered as 100 mm. Inside resonator, for the same reasons of improving laser output stability, a dielectric polarizer is inserted. The cylindrical LiF:F₂⁻ passive optical Q-switch cell is mounted approximately at one third of the laser resonator. The developed passively Q-switched Nd:YAG laser oscillator is operated at a repetition frequency of 10 pps (Hz).

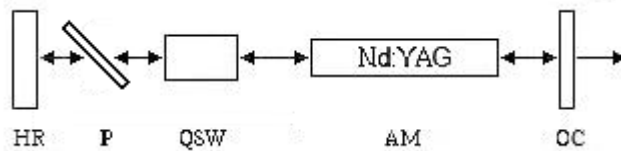


Fig. 8. Schematic representation of the investigated high brightness Nd:YAG laser setup developed for Sample C102. HR - High Reflectivity back mirror; P - Polarizer; QSW - LiF:F₂⁻ passive optical Q-switch cell; AM - active medium; OC - output coupler

The experiments were performed on three cylindrical LiF:F₂⁻ samples, denoted as C41, C75 and C102 with dimensions of $\varnothing 9$ mm and a length, l_a , of 30 and 47 mm. Two types of raw LiF crystals with different impurities concentrations content were processed using Co⁶⁰ γ and 7 MeV high energy electrons (denoted as “hee”) irradiation procedures in order to obtain F₂⁻ color centers inside them. In Table 1, the impurity content concentrations measured using Active Analysis method are presented. In Table 2, the irradiation procedures used for formation of F₂⁻ color centers are presented.

Table 1. The impurity content concentration of investigated LiF:F₂⁻ passive optical Q-switch samples.

Type	Impurity [ppm]									
	Na	Cl	K	Ca	Fe	Co	Sc	Zn	La	Pb
II.1	15	0.8	1.1	1.5	4	1.4	0.7	0.7	0.1	0.1
II.2	250	1.5	1.7	2.7	185	5.5	2.9	2.5	1.6	2.5

Table 2. The irradiation procedures for f₂⁻ color center formation used for investigated LiF:F₂⁻ passive optical q-switch samples.

Sam ple	Stage 1 [MRad]	Stage 2 [MRad]	Additional [MRad]
C41	150 Co ⁶⁰ γ	200 Co ⁶⁰ γ	8*48 Co ⁶⁰ γ
C75	100 “hee”	200 “hee”	6*48 Co ⁶⁰ γ
C102	200 “hee”	200 “hee”	10*48 Co ⁶⁰ γ

The end facets of the investigated LiF crystals were optically polished. Optical transmittance measurements were performed on the investigated LiF samples, before F₂⁻ color centers formation by irradiation procedures using a SPECORD 61 NIR (Carl Zeiss Jena) spectrophotometer. The optical transmittance of clean LiF samples was measured to be of ~0.90 - 0.92. In Table 3, the results of the spectroscopic measurements are summarized.

Table 3. The Spectroscopic Characteristics Of Investigated LiF:F₂⁻ Passive Optical Q-Switch Samples.

Sample	Type	l_a [mm]	T_{Lin}	T_{Lfin}	T_{PL}
C41	II.1	30	0.045	0.880	0.899
C75	II.2	47	0.040	0.853	0.865
C102	II.2	30	0.040	0.899	0.901

6. Experimental results

For both lines of experiments, three kinds of measurements are performed:

- Laser output energy (E_L [mJ]) versus pumping energy (E_P [J]) in free-running regime.
- Laser output energy (E_L [mJ]) versus pumping energy (E_P [J]) in passive optical Q-switching regime for single pulse ($N=1$) and double pulse ($N=2$) generation.
- Single pulse generation time shape, with a FWHM time duration estimation.

In the plots of Fig. 9 and 10, the experimentally observed variations of laser output energy in free-running (denoted as E_{Lfr}) and Q-switched (denoted as E_{Lqsw}) regimes versus pumping energy (denoted as E_P) are presented.

In the case of free-running regime, the experimentally measured values are linearly interpolated using the least square method such as:

$$E_{Lfr} [\text{mJ}] = A \times E_P [\text{J}] - B \quad (18)$$

From this equation of experimental data interpolation, the threshold value of pumping energy for free-running laser oscillation was deduced as:

$$E_{Pth_fr} = \frac{B}{A} \quad (19)$$

In equation (7) are indicated the measure units of laser output energy (E_{Lfr}) and pump energy (E_P).

It is considered as an information of interest the “extraction coefficient”, K_e , defined as the ratio of laser out-

put energy in Q-switched and free-running regimes for a given value of pumping energy:

$$K_e = \frac{E_{Lqsw}}{E_{Lfr}} \quad (20)$$

During the performed investigation on the LiF:F₂⁻ samples, K_e is defined for the Q-switching threshold value of pumping energy.

In Fig. 8 the experimentally observed laser output energy values for free-running and Q-switched during the experiments performed at Laser Department of INFLPR are presented. The free-running interpolation curve is defined as

$$E_L[\text{mJ}] = 29.410 \times E_p[\text{J}] - 315.301 \quad (21)$$

with threshold pumping energy estimated as:

$$E_{P_{th_fr}} = 10.7\text{J}$$

In the performed investigations, the dynamic slope of equation (10) was of interest in the sense of performance prediction. The observed value of A was considered as acceptable,

$$A_{LD} = 29.410$$

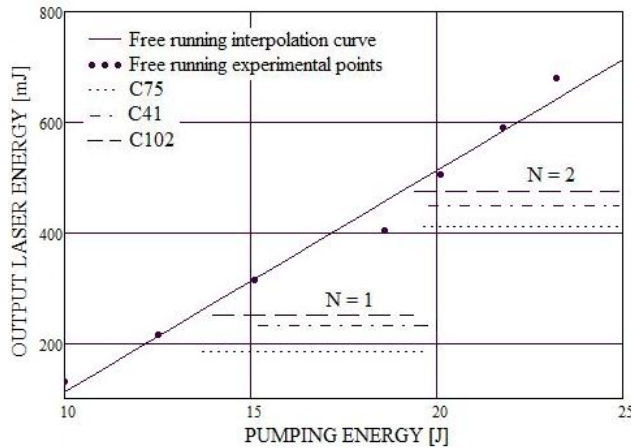


Fig. 9. The experimentally observed laser output energy values for free-running and Q-switched regimes, using the setup for Sample C75.

In Fig. 10 the experimentally observed laser output energy values for free-running and Q-switched during the experiments performed at CONTINUUM Laser Laboratories are presented. The free-running interpolation curve is defined as

$$E_L[\text{mJ}] = 40.151 \times E_p[\text{J}] - 290.054 \quad (22)$$

with threshold pumping energy estimated as:

$$E_{P_{th_fr}} = 7.2\text{J}$$

In the performed investigations, the dynamic slope of Eq. (11) was of interest in the sense of performance prediction. The observed value of A was considered more

than acceptable in comparison with the value observed at INFLPR Laser Department, being with ~30% greater, $A_{CL} = 40.151$

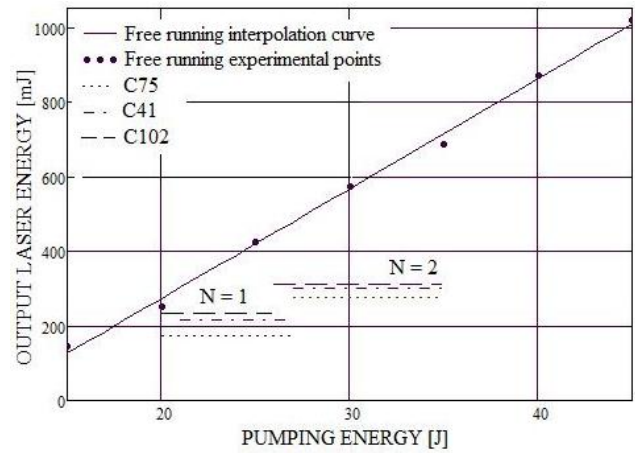


Fig. 10. The experimentally observed laser output energy values for free-running and Q-switched, using the setup for Sample C102.

In TABLE 4 the experimentally results observed during the experiments using the setup for Sample C75 are summarized.

Table 4. The experimentally observed results using the setup for sample c75.

Sample	$E_p[\text{J}]$	N	$E_L[\text{mJ}]$	K_e	$t_p[\text{ns}]$
C41	21-27	1	215	0.71	~ 4
	27-35	2	300		
C75	20-27	1	175	0.64	~ 4
	27-36	2	280		
C102	20-26	1	235	0.86	~ 4
	26-36	2	310		

In Table 5 the experimentally results using the setup for Sample C102 are summarized.

Table 5. The experimentally observed results using the setup for Sample C102.

Sample	$E_p[\text{J}]$	N	$E_L[\text{mJ}]$	K_e	$t_p[\text{ns}]$
C41	15.2-20	1	235	0.73	~ 4
	20-25	2	450		
C75	13.7-20	1	185	0.71	~ 4
	20-25	2	400		
C102	13.8-19	1	250	0.95	~ 4
	19-25	2	475		

In Fig. 11, the experimentally measured for the “worst” case of C75 Q-switch sample laser single pulse time shape is presented. The observed FWHM single laser pulse time duration is estimated as ~ 5 ns. The peak power of single laser pulse is estimated as 37 MW. The similar value for the “best” case of C102 Q-switch sample is estimated to be ~50 MW.

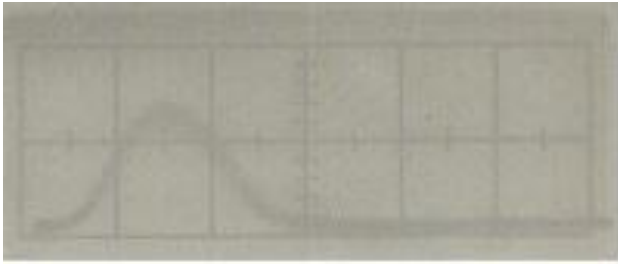


Fig. 11. The experimentally measured laser single pulse time shape for Sample C75 is presented. Horizontal time division is 2ns.

7. Conclusions

The presented experimental and numerical simulation results, which are in good agreement, less than 10% relative differences can be considered as a validation of developed low cost non-sophisticated computer programs dedicated to the proposed target. The developed laser numerical simulation computer programs are suitable for further improvements. As a first step in development of a laser simulation software package, the presented experimental and numerical simulation can be used for an improved design of high brightness passively optically Q-switched laser oscillators.

References

- [1] A. E. Siegman, Lasers, Chapter 26 (University Science, Mill Valley, Calif., 1986).
- [2] C. J. Mercer, Y. H. Tsang, D. J. Binks, Journal of Modern Optics, 1362-3044, **54**(12-15) 1685 (2007).
- [3] Koechner W. Solid State Laser Engineering, 6th ed.1999. Berlin, Springer. 2006.
- [4] Degnan J. IEEE journal of quantum electronics; **5**(2), 214 (1989).
- [5] G.Phillipps, K.Mundt, J.Vater, I. Lancranjan, Romanian Journal of Optoelectronics **5**(3), 33 (1997).
- [6] Y. K. Kuo, M. Birnbaum, W. Chen, Appl. Phys. Lett. **65**, 3060 (1994).
- [7] Y. K. Kuo, M. F. Huang, M. Birnbaum, IEEE J. Quantum Electron. **31**, 657-663 (1995)
- [8] Y. K. Kuo and M. Birnbaum, Appl. Phys. Lett. **67**, 173-175 (1995).
- [9] Y. K. Kuo, M. Birnbaum, Appl. Opt. **35**, 881 (1996).
- [10] Y. K. Kuo, W. Chen, R. D. Stultz, M. Birnbaum, Appl. Opt. **33**, 6348 (1994).
- [11] Y. K. Kuo, M. Birnbaum, F. Unlu, M. F. Huang, Appl. Opt. **35**, 2576 (1996).
- [12] Y. K. Kuo, S. Lee, F. Unlu, M. F. Huang, M. Birnbaum, P. D. Fuqua, B. Dunn, Electron. Lett. **32**, 2146 (1996).
- [13] Y. K. Kuo, H. M. Chen, Jpn. J. Appl. Phys. **39**, 6574 (2000).
- [14] Y. K. Kuo, H. M. Chen, J. Y. Chang, Opt. Eng. **40**, 2031 (2001).
- [15] Y. K. Kuo, H. M. Chen, Y. Chang, Appl. Opt. **40**, 1362 (2001).
- [16] I. Lancranjan, The Formation of F₂⁻ Color Centers in Lithium Fluoride Crystals by Gamma, Electron and Neutron Irradiation, Atomic Physics Institute Scientific Report -Preprint CS-14, 1989
- [17] S. Dong, Q. Lü, I. Lancranjan, Optics & Laser Technology, **25**(3), 175 (1993).
- [18] J. J. Degnan, IEEE J. Quantum Electron. **25**, 214 (1989).
- [19] J. J. Zayhowski, P. L. Kelley, IEEE J. Quantum Electron. **27**, 2220 (1991).
- [20] T.T.Basiev, S.B.Mirov, V.V.Osiko, IEEE J. of Quantum Electronics, **24**, 1052 (1988).
- [21] I. Lancranjan, S. Miclos, D. Savastru, A. Popescu, J. Optoelectron. Adv. Mater. **12**(12), 2456 (2010).
- [22] I. Lancranjan, S. Miclos, D. Savastru, A. Popescu, J. Optoelectron. Adv. Mater. **12**(8), 1636 (2010).

*Corresponding author: j_j_f_l@yahoo.com